Paper Title: Effects of particle buoyancy, release location, and diel vertical migration on exposure of marine organisms to microplastics in Delaware Bay

Authors: R. Alan Mason, Tobias Kukulka, Jonathan H. Cohen

Abstract:

Plastics are ubiquitous in the global ocean and present a potential hazard to marine organisms. One challenge in assessing the impact of plastics on marine organisms is calculating their exposure to the background plastics field. Guided by observational data of marine organisms and microplastics in the Delaware Bay, this study applies a rational approach for determining exposure times based on a hydrodynamic model of the Delaware Bay paired with particle tracking. We consider two different marine organism behaviors, organisms that stay at the surface and those that exhibit diel vertical migration (DVM), as well as different release locations in the bay in order to understand the spatial variability in microplastics exposure. Microplastics are either assumed to be neutrally-buoyant or surface-trapped, so that they either move with the full three-dimensional estuarine circulation or only with the surface currents. Total exposure time is then determined from the modeled time-integrated background microplastics concentrations for each simulated marine organism path. Exposure was found to be greatest for surface-trapped organisms exposed to surface-trapped plastics as they both tend to aggregate in tidelines. DVM limits exposure to plastics by removing organisms from the surface-trapped plastics field. For neutrally-buoyant plastics, surface-trapped organismal exposure time greatly depends on the organism release location. Exposure

is modified by two competing DVM influences: Lesser plastic concentrations at depth decrease the exposure, whereas limiting motion toward the mouth of the bay where the plastic concentrations are smaller increases the exposure. Marine organism exposure to microplastics in a dynamic estuarine environment greatly depends on plastic buoyancy and an organism's vertical position. Both of these factors need to be taken into account for comprehensive microplastic impact studies.

Keywords: Microplastic pollution; marine debris; zooplankton; estuarine dynamics; plastics exposure; risk assessment; USA; Delaware Bay

1 – Introduction:

Microplastics are an emerging pollutant throughout the global ocean (Law 2017, Ostle et al. 2019). Plastics are estimated to be 60 to 80 percent of all marine debris and greater than 90 percent of all floating debris (US EPA 2016). Plastics are lightweight and can be transported by wind and ocean currents (Law 2017) and dispersed vertically by wind stress, wave-driven mixing, as well as heat fluxes (Kukulka et al. 2012, Brunner et al. 2015, Kukulka et al. 2016). Plastics can also spread throughout the water column based on their density, which is influenced by plastic type, trapped air content, and biofouling (Andrady 2011, US EPA 2016, van Sebille et al. 2020). Plastics are typically broken into two size categories, macroplastics, size greater than 5mm, and microplastics, size smaller than 5mm, with microplastics being the more abundant of the two (Law 2017, US EPA 2016).

While microplastic concentrations in the open ocean can be on the order of 10^6 pieces km^{-2} (Law et al. 2010, Law et al. 2014), several studies, such as Yonkos et al. (2014), Gray et al. (2018), Sutton et al. (2016), Cohen et al. (2019), Bikker et al. (2020), have found that microplastics can be in higher concentrations in estuaries than in the open ocean. The high concentrations of plastics in estuaries, as well as the ease of transport of plastics, greatly increases the chance for a harmful interaction for an organism with plastics, such as ingestion (Wright et al. 2013, Law 2017, Botterell et al. 2020). Due to the small size of microplastics, they could be consumed by smaller organisms, such as zooplankton, and present a potential entry point for plastics into the food web (Wright et al. 2013, Vermeiren et al. 2016, Van Colen et al. 2020).

One way to assess the impact of microplastics on zooplankton is through the use of a risk assessment. Risk assessments are calculated as the exposure to the hazard times the adverse response to the hazard, which is a function of exposure (Law 2017). One of the great challenges in using a risk assessment is quantifying the exposure and the adverse response (Law 2017). In this study, we propose a rational approach for determining exposure times in the Delaware Bay based on a hydrodynamic model paired with particle tracking.

The Delaware Bay was selected as our study site due to the recent microplastics (Cohen et al. 2019) and zooplankton (Wickline 2016) observational studies done in the region. The Delaware Bay, located in the mid-Atlantic region, is part of the Delaware Estuary and extends roughly 75 km from the estuary mouth (Garvine 1991). The Delaware Estuary is one of the largest estuaries in the United States and extends 215 km from the limit of tidal influence near Trenton, NJ to the mouth of the Delaware Bay (Sharp 1983). The Delaware River is the largest

source of freshwater to the system with a yearly average of 330 m^3 s^{-1} (Sommerfield and Wong 2011). While the average depth of the bay is 8 m (Wong and Münchow 1995), regions associated with the ancestral river channel can have depths greater than 30 m (Garvine 1991, Whitney and Garvine 2006). The largest tidal velocities in the Delaware Bay, approximately 90 cm s^{-1}, are associated with this channel near the mouth of the bay (Münchow et al. 1992). In the upper Delaware Bay and the region just up-estuary, the estuary is relatively narrow and the estuarine exchange flow and salt flux occur predominantly near the center of the estuary in the ancestral river channel and is negligible on the flanks (Aristizabal and Chant 2013, Geyer et al. 2020). In the mid and lower bay, the bay widens considerably to 45 km across at its widest point and 18 km across at the mouth. This width results in the estuarine circulation being influenced by planetary rotation (Whitney and Garvine 2005, Li et al. 2014). Most notably, planetary rotation causes the separation of fresher water toward the right (west) side of the estuary and leads to the fresher water not interacting with the more eastern part of the estuary (Whitney and Garvine 2005, Li et al. 2014). This separation can drive buoyancy-driven flows and river plumes (Whitney and Garvine 2005, Whitney and Garvine 2006, Li et al. 2014, Horner-Devine et al. 2015). Cross-channel circulation, driven by mechanisms such as differential advection (Lerczak and Geyer 2004), is vital in the Delaware Bay for maintaining stratification, net shear flow, and salt flux (Aristizabal and Chant 2013, Geyer et al. 2020). The cross-channel circulation can also result in tidelines. Tidelines are bands that form at the center of converging surface currents, which are driven by mechanisms such as axial convergence and differential advection (Nunes and Simpson 1985, Lerczak and Geyer 2004, Geyer et al. 2020) or mixing along strong density gradients (O'Donnell 1993, MacCready and Geyer 2010, Horner-Devine et

al. 2015). The converging surface currents transport passive buoyant organisms and debris, such as flotsam and plastics, into the tidelines and lead to increasing concentrations over time (Nunes and Simpson 1985, MacCready and Geyer 2010). The accumulation of plastics in these bands could result in the high hot spot plastics concentrations proposed by Cohen et al. (2019) for the Delaware Bay. This dynamic estuarine environment is ideal for investigating zooplankton exposure to microplastics.

Diel vertical migration (DVM) is a wide-spread behavior in zooplankton and micronekton that describes the movement of being near the surface at night and then migrating to depth during daylight hours (Lampert 1989, Hays 2003). DVM behavior serves to give these organisms a refuge from visual predation at depth during the day and nighttime access to food in surface waters (Lampert 1989, Cohen and Forward 2009).

This study is aimed at providing a proof-of-concept to illustrate that marine organism exposure to microplastics in an estuary greatly depends on plastic buoyancy and the organism's DVM. Given our limited scope, we examine a typical exposure based on selective and representative concrete examples that are motivated by recent observational data of zooplankton and microplastics in Delaware Bay. Specifically, the study examines two zooplankton behaviors (with and without DVM) and two extreme microplastics buoyancies (neutrally-buoyant and surface-trapped) at common locations in Delaware Bay.

2 – Methods:

2.1 – Hydrodynamic model of the Delaware Bay:

We utilize an existing validated model of the Delaware Bay (Castellano and Kirby 2011, Kukulka et al. 2017) that is an application of

the Regional Ocean Modeling System (ROMS) (ROMS, Haidvogel et al. 2000, Shchepetkin and McWilliams 2005) within the Coupled-Ocean-Atmospheric-Wave-Sediment Transport (COAWST) Modeling System (Warner et al. 2010). Similar models have been successfully utilized in the Delaware Bay for a wide variety of studies such as plastic distribution (Cohen et al. 2019), salt flux (Aristizábal and Chant 2013, Geyer et al. 2020), river plume dynamics (Whitney and Garvine 2006, Jurisa and Chant 2013), circulation dynamics (Geyer et al. 2020), sediment transport (McSweeney et al. 2017), and bivalve distribution (Hoffman et al. 2009).

The modeling domain includes portions of the upper Delaware Estuary and extends out to the continental shelf break. The model utilizes a curvilinear grid with the highest resolution near the mouth of the bay, 0.75 km – 2.0 km, and the coarsest resolution at the shelf break, 8 km, with 10 terrain-following depth layers. As discussed in Kukulka et al. (2017), this resolution is sufficient to accurately simulate the key circulation features of the region. The model is forced by realistic forcings for tide, freshwater discharge, and wind. The tide is forced by tidal constituents from the ADCIRC tidal database and is applied to the open boundaries of the grid (Luettich et al. 1992, Kukulka et al. 2017). The constituents used are M2, S2, M4, M6, K2, K1, N2, O1, and Q1, with M2 being the chief constituent for the region (Castellano and Kirby 2011, Kukulka et al. 2017). The freshwater discharge imposed in the model is based on observational data gathered from the Delaware River gauge at USGS site 01463500 at Trenton, NJ. The Delaware River accounts for 58% of freshwater input into the bay. Other than the Delaware River, only the Schuylkill River (15%) and Christina River (5%) account for more than one percent of freshwater to the bay (Sharp 1983). As the Schuylkill and the Christina converge with the estuary upstream of the salt intrusion, they can be simulated as entering the estuary at

the same point as the Delaware River without loss of dynamics (Whitney and Garvine 2005, Aristizábal and Chant 2013). The observational data from the USGS site is then upscaled to represent the full value of freshwater entering the estuary (Whitney and Garvine 2005). Surface wind stress could be readily included in the model, such as in Kukulka et al. (2017) and Cohen et al. (2019), but is turned off in this study to focus on the effect of organism behavior, particle buoyancy, and release location.

The model time frame used is June 2, 2017 to June 12, 2017. Early to mid-June was selected because both the field observations for the zooplankton (Wickline 2016) and the microplastics (Cohen et al. 2019) occurred during this time frame. The year 2017 was selected to correspond to the year of the microplastics sampling. In addition to turning off the wind, we also set the river discharge to be constant at the yearly average to better focus on organism behavior, particle buoyancy, and release location. The model is started several months prior to this time to allow sufficient time for model spin up.

2.2 – Marine Organism: We consider the zooplankton as Lagrangian passive tracers moving with the velocity field simulated by the ROMS model. One advantage of representing the zooplankton in this fashion is that we can generalize the tracers to any marine organism that exhibits passive movement. To reflect this, hereafter we refer to the zooplankton simply as marine organisms. We also consider two different behaviors for the marine organisms, a DVM behavior and a non-migrating, surface-trapped behavior. We account for the DVM behavior in the tracer by changing the velocity field from the surface currents to the near-bottom currents during daylight hours. Note that this idealized representation of DVM does not

capture potential vertical mixing effects, which are beyond the scope of this study. For the surface-trapped behavior, the organisms are only exposed to the surface current velocities.

The marine organism release locations were based primarily on observational data of *Acartia tonsa*, the dominant zooplankton species in the Delaware Bay (Cronin et al. 1962, Wickline 2016). *Acartia tonsa* is found to have high abundances throughout the bay in June, with slightly higher values in both the upper bay and near the mouth of the bay (Wickline 2016). Based on this, we elected to have release locations in these two general areas. The upper bay location (Figure 1A, white circle) was selected to coincide with the sampling point that had the highest *Acartia tonsa* abundances in the spring since the June abundance distribution was similar across several sampling points in the region (Wickline 2016). The lower bay release location (Figure 1A, red circle) was selected to coincide with the location of the highest overall zooplankton abundances for the early summer (Wickline 2016). The organisms are initialized randomly near the initial release location, within 0.2 km, in order to account for the different possible trajectory paths in the area. The marine organism path is allowed to develop for 10 days in order to capture the exposure over the course of a typical lifetime for *Acartia tonsa* (Leandro et al. 2006). The exposure for each of the 100 organisms is calculated and then averaged over the 100 organisms to find the average exposure for an organism released either in the lower or upper bay. To study the spatial variability of exposure in the bay, organisms are also initialized with an evenly spaced full bay distribution and allowed to develop for 10 days. The total exposure for each organism is calculated and then plotted at its initial location to examine the exposure distribution.

2.3 – Microplastics: In addition to considering marine organisms, we also consider the movement of microplastics. We first consider a neutrally-buoyant plastics field that is allowed to move with the full three-dimensional estuarine circulation. We set the neutrally-buoyant plastics field to be inversely related to salinity. This assumption is based on the observational data presented in Cohen et al. (2019). In both sample months, April and June, the plastics concentrations were highest in the upper estuary and decreased toward the mouth of the bay (Cohen et al. 2019). In the month of June, the highest observed plastics concentration was 4.8 piece m^{-3}, which we associate with a salinity of 0, and there were several low observed plastics concentrations in the lower bay at approximately 0.1 piece m^{-3}, which we associate with a salinity of 35 (Figure 1A).

Second, we consider highly positively-buoyant plastics that remain surface-trapped throughout the course of the simulation (Kukulka et al. 2012). This plastics field is represented in the same manner as the surface-trapped marine organisms. Similarly to the neutrally-buoyant plastics, surface-trapped plastics are assumed to enter the bay only due to freshwater input from the Delaware River. These plastics are initialized in the far upper bay region of the study area at a rate of once every 3 hours beginning 30 days prior to the initialization of the organisms to allow sufficient time for the plastics field to spin up. A persistent feature of the plastics field is that it quickly converges to tidelines and is transported toward the mouth of the bay in these tidelines (Figure 1C). The surface-trapped plastics field is also scaled based on the data presented in Cohen et al. (2019). However, we use the estimated value for the highest concentration inside a tideline, $9x10^4$ piece m^{-3}, since none of the observational data in Cohen et al. (2019) was taken within a tideline. The highest microplastics concentration occurrence in

our model was set to $9x10^4$ piece m^{-3} and all other concentrations were scaled between this and a background concentration of 0.1 piece m^{-3}. As explored in Cohen et al. (2019), smaller unresolved turbulence can smear the sharp gradients of plastic hot spots, but do not qualitatively alter the results. Thus, we do not include the effects of unresolved turbulence on particle tracking in this study.

2.4 – Exposure Calculation: Two different exposure calculations are presented in this paper. The first is an instantaneous exposure, representing the exposure level at each time point. This is determined from the model using the background microplastics concentrations for each simulated marine organism path. The second is a net exposure, representing the cumulative exposure from organism release to the current time point for each simulated marine organism path over the course of the 10-day simulation. The net exposure is calculated as the time integral of the instantaneous exposure.

3 – Results and Discussion:

The organisms released at the same location in the bay with different behaviors initially have similar paths, but these paths diverge over the course of the simulation (Figure 1A). Both organism behaviors initialized in the lower bay are first transported outside of the bay on the fourth day, June 6, but are moved by tides in and out of the bay until the DVM organisms fully exit the bay on the sixth day, June 8, and the surface-trapped organisms on the seventh day, June 9. The DVM organisms at the upper bay location exit the bay on the seventh day, while the surface-trapped organisms remain in the bay for the entire simulation. This is despite the

surface-trapped organisms being transported approximately 27 km after two days and 50 km after four days toward the mouth of the bay compared to DVM organisms being transported approximately 15 km after two days and 30 km after four days. The path and transport of the DVM organisms can best be described by the phase of the tidal currents while they are at the surface. Since the M2 tidal period is 12.42 hours, the DVM organisms migrate to the surface at an earlier point in the tidal cycle than when they migrated to the surface the previous day. At the beginning of the simulation, the DVM organisms migrate to the surface an hour prior to the beginning of flood tide and migrate to the bottom just before the max ebb tide and experience slight transport up-estuary since they stay longer at the surface during flood than ebb tide. This slight up-estuary transport can be seen in both release locations but is slightly more pronounced in the lower estuary organisms (Figure 1A). As the simulation progresses, the DVM organisms shift to be at the surface longer during ebb tide than flood tide. Another important factor is the diurnal inequality in the tidal signal that is the result of the interaction of the principal constituents and higher harmonics (Friedrichs and Aubrey 1988, Nidzieko 2010). As the diurnal inequality becomes more prominent leading into spring tide on the eighth day of the simulation, the higher high water occurs at night and the lower high water occurs in the afternoon. The DVM organisms migrate to the surface just after the higher high water point and experience a greater tidal range during ebb tide than flood tide. This inequality in tidal velocity also leads to a net transport down-estuary. Additionally, the position of where the particle converge near the mouth of the bay can lead to trapping in the estuary. The surface-trapped particles converge to the center of the mouth, which is an area that leads to trapping in the Delaware Bay (Figure 1A and 1C). Conversely, the DVM organisms reach the mouth of the bay

toward the southwest shore (near the state of Delaware) where the outflow is stronger due to the deflection of currents by the Coriolis force (Whitney and Garvine 2005), which can lead to the organisms exiting the bay.

If the vertical mixing is sufficiently weak, the bottom of the water column in the Delaware Bay is saltier than the surface (Figure 1B). The salinity differences between the surface and the bottom of the water column are greatest near the deep channel in the center of the bay as well as near the western shore of the bay. The salinity difference on the western shore of the bay are due to the river discharge being deflected by planetary rotation to this area and resulting in fresher surface waters (Whitney and Garvine 2005). The peak salinity difference between the surface and the bottom of the water column is nearly ten, which would result in a neutrally-buoyant plastics exposure differential of 1.34 piece m^{-3} between the surface and the bottom.

Similar to the modeled plastics field in Cohen et al. (2019), the surface-trapped plastics quickly form a patchy, inhomogeneous distribution in the Delaware Bay (Figure 1C). The largest plastics concentrations occur near the center axis of the estuary and are found in tidelines. Outside these tidelines, the plastics concentrations are much smaller.

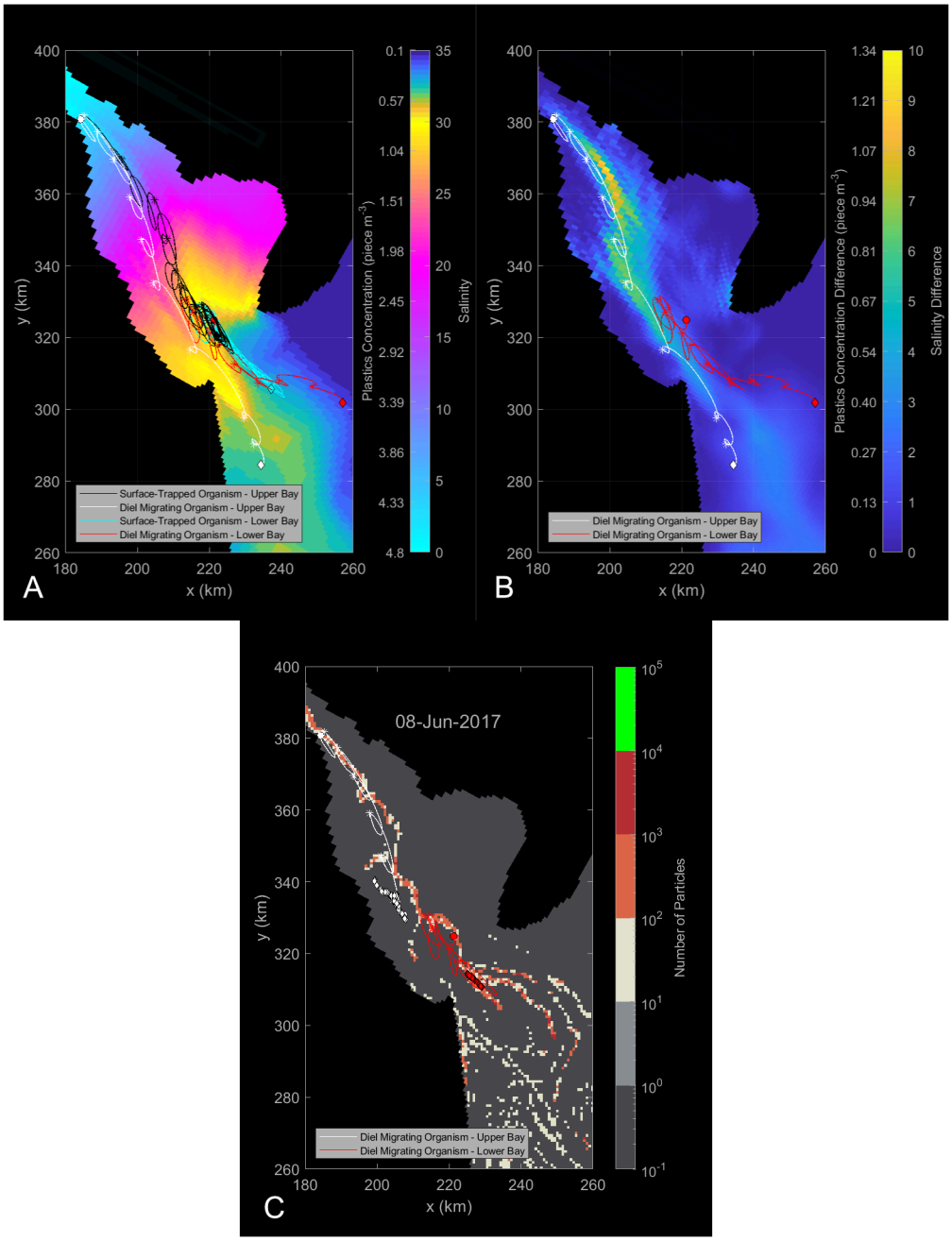

Figure 1: Time-dependent organism paths and instantaneous background plastics concentrations for different cases: (A) neutrally buoyant plastics, (B) difference between bottom and surface plastics concentrations, and (C) surface-trapped plastics concentrations. Paths are shown for release locations in the upper bay (black and white lines) and lower bay (cyan and red lines) for organisms with DVM (white and red lines) and without DVM (cyan and

black lines). The initial organism location is represented by a circle, a daily position update is given by the asterisk, and the final location after the 10-day simulation is represented by the diamond. The salinity field for (A) and (B) is time averaged over the entire simulation. The plastics field shown in (C) is a snapshot of the plastics field at midnight on June 8, 2017.

Exposure to plastic concentrations changes as the organisms move through the bay (Figure 2). This is the case for all organism behaviors and release locations exposed to the neutrally-buoyant plastics field (Figure 2A) and the surface-trapped plastics field (Figure 2B). In determining the exposure to the neutrally-buoyant plastics field, the key factor is the location in the bay. The organisms that begin further up the bay are exposed to much higher plastics concentrations during the simulation than organisms that begin closer to the mouth of the bay (Figure 2A), leading to a higher net exposure to plastics (Figure 3A). As can be seen in Figures 2A and 3A, DVM can result in two competing influences on exposure to the neutrally-buoyant plastics. The first is by decreasing exposure as organisms migrate to saltier water near the bottom of the water column (Figure 1B). This effect can be observed in Figure 2A for both release locations. The effect is most dramatic on June 4 for the lower bay organisms, exposure increases by nearly 1.0 piece m^{-3} after migrating to the surface and a decrease by over 0.5 piece m^{-3} after migrating to depth, and June 6 for upper bay organisms, exposure decreases by nearly 1.0 piece m^{-3} after migrating to depth. The second influence of DVM is that it can limit organism movement toward the mouth of the bay based on the correlation of when they are at the surface and the tidal phase. This can be observed in the difference in transport of the upper estuary organisms during the first four days of the simulation. This results in organisms

remaining in fresher water with higher plastic concentrations for a longer period of time (Figure 1A). This effect can be observed in the upper bay organisms as the decrease in exposure is more gradual for the DVM organisms than the surface-trapped organisms (Figure 2A). This limiting of horizontal movement in the bay is similar to the results found by Kimmerer et al. (2014) who studied the effects of vertical migration on plankton retention in the San Francisco Bay. The competing effects of DVM can also be seen in the organisms' net exposure (Figure 3A). DVM in the upper bay leads to a higher net plastics exposure due to a longer amount of time spent in fresher waters with higher plastics concentrations in the upper bay (Figure 1A). In the lower bay, both effects of DVM can be observed in the first several days (Figure 3A). The initial net exposure for the DVM organisms is less than that of the surface-trapped organisms due to migration to the bottom of the water column, but then becomes greater due to slower movement toward the mouth of the bay during the first several days of the study period.

In determining the exposure of organisms to surface-trapped plastics, we need to consider the spatial distribution of the plastics field itself (Figure 1C). The surface-trapped plastics converge to tidelines near the center axis of the bay, which results in inhomogeneous patches of plastics that can vary both in the along-channel and cross-channel directions (Cohen et al. 2019). The cross-channel variation in plastics concentration is the greater of the two with very high concentrations of plastics in the tidelines and background plastic concentrations just a few kilometers away on either side of the tideline (Figure 1C). In the along-channel direction, plastic concentrations in the tidelines/hotspots are greater near the mouth of the bay than further up the bay (Figure 1C). The tidelines near the mouth of the bay are likely positioned by axial convergence to be over the saltier ocean water brought in by the high tidal velocities in

the deep central channel. In this position, the tidelines are located outside the region of heightened outward-flow influenced by the freshwater discharge, which can lead to the trapping of particles near the mouth of the bay and higher plastics concentrations in this region than in the upper bay. In contrast, the neutrally-buoyant plastics field varies only with the salinity gradient and predominantly in the along-channel direction (Figure 1A). The marine organism behavior is also important in determining exposure to surface-trapped plastics as DVM removes organisms from the surface-trapped plastics field while they are at depth. This removal from the surface-trapped plastics field leads to large changes in exposure for the DVM organisms (Figure 2B) and the step-like increases in the net exposure curve (Figure 3B). At depth, the organisms are still subjected to the background plastics concentration, 0.1 piece m^{-3}, which can lead to times of similar exposure between the two initial organism locations (Figure 2B). Conversely, surface-trapped organisms remain trapped within a tideline after converging. Since the surface-trapped organisms and the marine debris converge to similar tidelines, the surface-trapped organisms are exposed to high levels of plastics throughout the simulation, resulting in very high levels of instantaneous exposure (Figure 2B) and net exposure (Figure 3B). The net exposure for organisms with the same behaviors is similar between the upper and lower bay locations (Figure 3B). The upper and lower bay initial locations are near tidelines and indicate that the initial position near the tideline is more important than the initial along-channel location in determining exposure to surface-trapped plastics. Additionally, the organisms exhibiting DVM had a net exposure that was an order of magnitude less than the surface-trapped organisms, indicating that DVM behavior is important in determining net exposure to surface-trapped plastics.

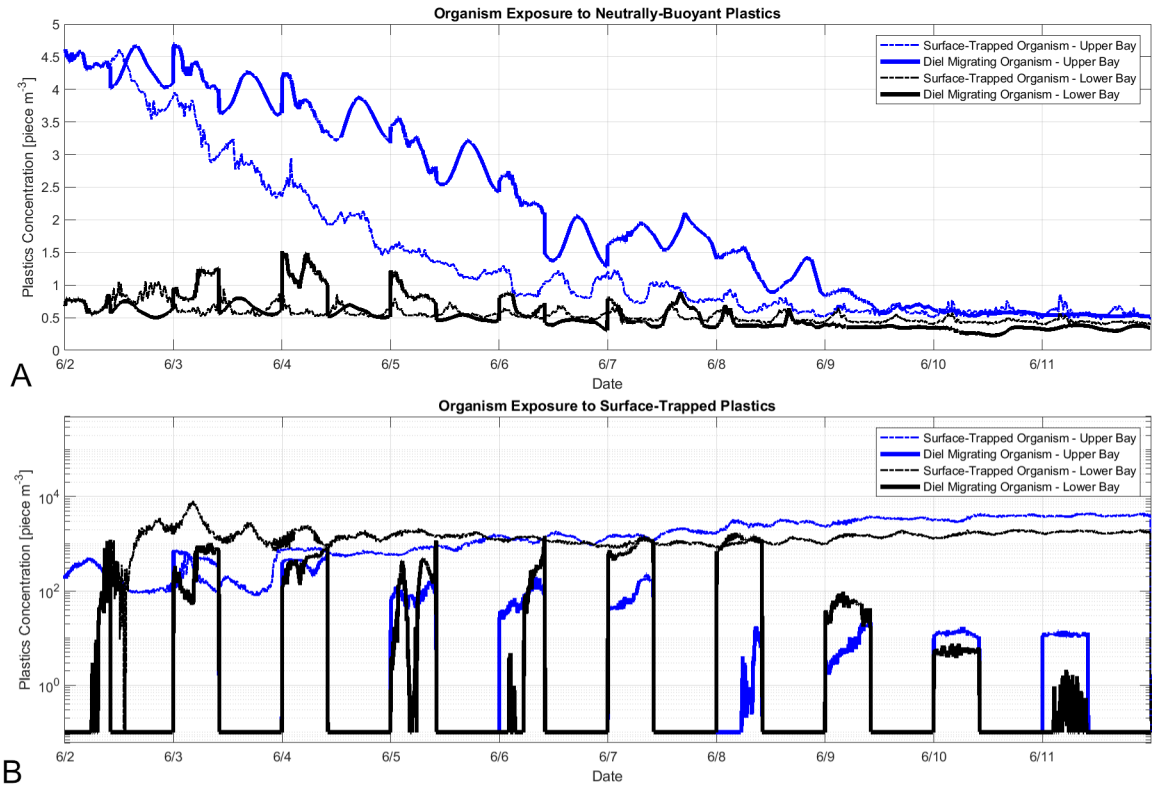

Figure 2: Exposure of organisms to (A) neutrally buoyant plastics and (B) surface-trapped plastics for organisms without DVM (thin-dashed lines) and those with DVM (thick lines) in the upper bay (blue lines) and the lower bay (black lines). Plastic concentrations are scaled according to the data presented in Cohen et al. (2019). The background concentration for both plastics fields is set to 0.1 piece m^{-3}. The highest plastics concentrations are set to 4.8 piece m^{-3} for the neutrally-buoyant plastics and $9x10^4$ piece m^{-3} for the surface-trapped plastics.

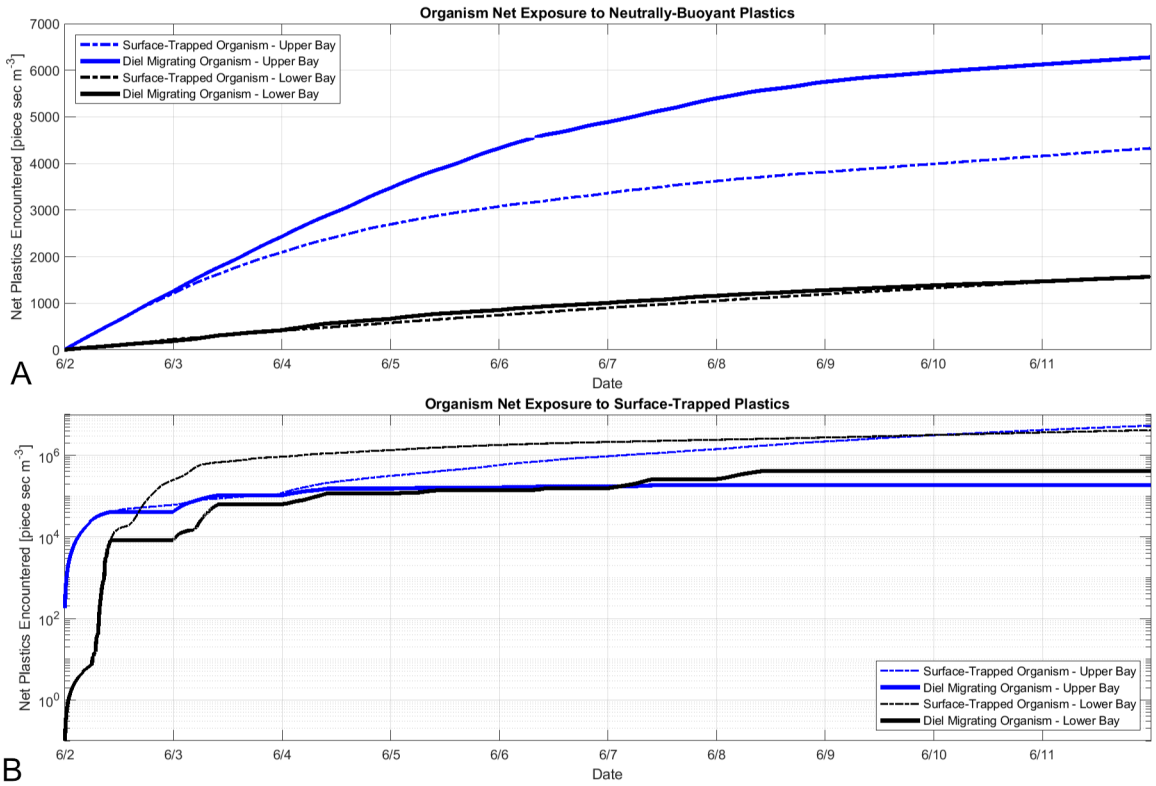

Figure 3: Net exposure levels of organisms to (A) neutrally buoyant plastics and (B) surface-trapped plastics for organisms without DVM (thin-dashed lines) and those with DVM (thick lines) in the upper bay (blue lines) and the lower bay (black lines). Plastic concentrations are scaled according to the data presented in Cohen et al. (2019). The background concentration for both plastics fields is set to 0.1 piece m^{-3}. The highest plastics concentrations are set to 4.8 piece m^{-3} for the neutrally-buoyant plastics and $9x10^4$ piece m^{-3} for the surface-trapped plastics.

An interesting feature in Figure 2B is the variation in exposure levels between times when the DVM organisms are at the surface of the water column in the surface-trapped plastics field. To investigate this, we consider fixed points in the bay near the initial location for both the upper bay organisms and the lower bay organisms at the surface of the water column. The

neutrally-buoyant plastics field exposure for a fixed-point remains constant over time with regular variations of about 0.5 piece m^{-3} due to tidal motions. The upper bay exposure varies around 4.5 piece m^{-3} and lower bay varies around 0.75 piece m^{-3} exhibiting the along-channel plastics gradient that leads to the exposure difference between the two initial locations. The fixed-point surface-trapped plastics field exposure is much more variable in time (Figure 4). The surface-trapped plastics exposure changes by up to four orders of magnitude due to the positioning and movement of the tidelines (Figure 1C). The exposure to surface-trapped plastics in the lower bay shows a similar sudden increase and decrease as the tidelines pass over the release location. However, the events are more spread out due to the wider width of the lower bay and the change in exposure can be about five orders of magnitude due to higher concentrations of plastics in this region (Figure 1C). These large changes in exposure due to tideline positioning can explain the changes in exposure observed in Figure 2B between times the DVM organisms are at the surface. While at depth, the DVM organisms are transported at slower velocities than plastics trapped at the surface. This difference in velocity can result in a separation of plastics and organisms.

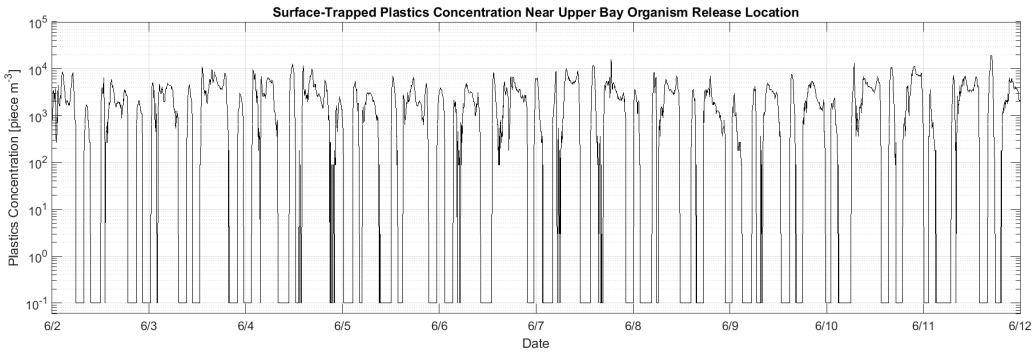

Figure 4: Variation in plastic concentrations surface-trapped plastics at a fixed point near the starting locations of the upper bay organisms.

To examine the variability in exposure caused by the initial release location, we study the final net exposure of organisms that are initially evenly-distributed throughout the bay (Figure 5). The final net exposure of the organism to plastics in Figure 5 is plotted at the organism's initial location. The full bay distribution of exposure to neutrally-buoyant plastics can be explained by a combination of the along-channel salinity gradient and the across-channel variability in currents (Figure 5A and 5B). The currents are faster closer to the deep channel. The faster currents result in particles initially located near the deep channel to experience more rapid movement down-estuary toward saltier water with lower plastics concentrations than particles initially located closer to shore. Due to the limitation of horizontal movement caused by DVM during this time frame, the effect of DVM is a shift in the distribution of higher net exposures closer to the mouth of the bay (Figure 5B). The effects of DVM when organisms are at the surface during other tidal phases is considered further in the sensitivity study. DVM also increases the highest exposure level in the bay from 8748 piece sec m^{-3} to 10197 piece sec m^{-3} as well as increases the average exposure in the bay from 2945 piece sec m^{-3} to 3983 piece sec m^{-3}.

In contrast, the cross-channel proximity of the initial location of the organism to the tideline is more important in determining exposure to the surface-trapped plastics (Figure 5C and 5D). As can be seen in Figure 5, the net exposure levels are similar in the along-channel direction but vary in the cross-channel direction. This variation in the cross-channel direction is

due to greater amounts of time needed for the organisms to be transported and converge to a tideline. The lower exposure levels on the state of Delaware side of the bay are due to the effects of planetary rotation on the estuarine circulation. The exposure levels to surface-trapped plastics for the non-migrating organisms is greater than that of the DVM organisms throughout the bay. This is also reflected in the difference between both the highest exposure level in the bay (20694764 piece sec m^{-3} compared to 2418607 piece sec m^{-3}) and the bay-wide average (2593248 piece sec m^{-3} compared to 282741 piece sec m^{-3}) being an order of magnitude higher for the non-migrating organisms than the DVM organisms.

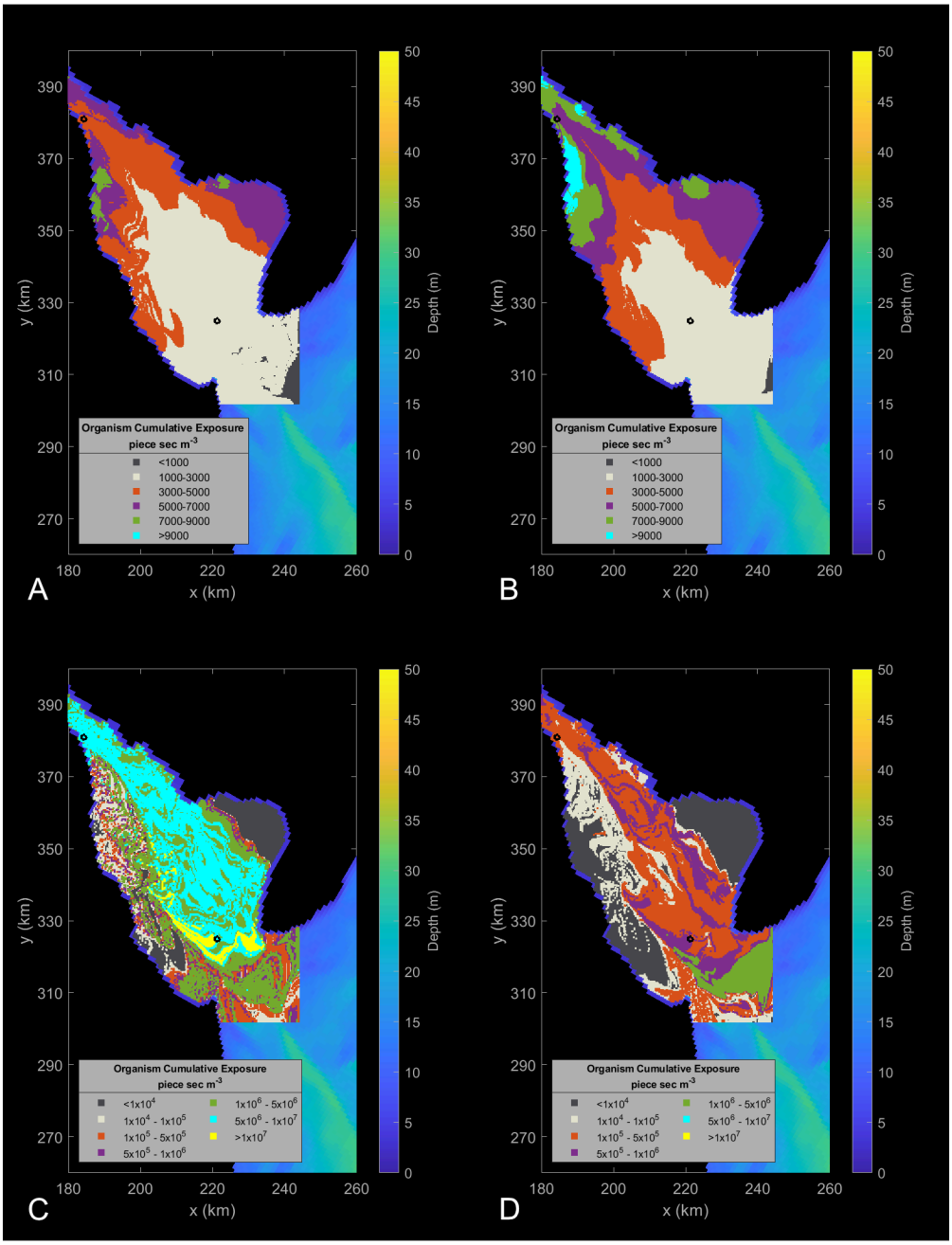

Figure 5: Full bay initial distribution of surface-trapped organisms (A and C) and DVM organisms (B and D) exposed to neutrally-buoyant plastics (A and B) and surface-trapped plastics (C and D). The final net exposure is plotted at the initial location of the organism. The black circles indicate the release locations for the upper and lower bay organisms.

To better understand the influence of the tidal phase, we run sensitivity experiments releasing organisms at highwater point, max flood tide, low water point, and max ebb tide in the tidal cycle. Additionally, we test these release locations during both spring tide and neap tide. For all cases, the features and variability in exposure discussed in this paper remain consistent. While there are some differences in the exact exposure level depending on the case, these differences are minor by the end of the 10-day simulation for all cases except for exposure of DVM organisms to surface-trapped plastics in the lower bay. For this case, the different release points in the tidal phase result in a different initial distance away from the nearest tideline. These different initial distances resulted in differing convergence times to the tideline and thus larger differences in the exposure level due to the patchy, inhomogeneous nature of the surface-trapped plastics field. While this effect is also present in the other surface-trapped plastics cases, it is less pronounced in the upper bay due to its narrower width and for the surface-trapped organisms in the lower bay since they remain in the surface current field. Additionally, greater transport of DVM organisms is observed during spring tide. However, the motion of the transport is still the result of the dominant tidal phase. While the organisms are at the surface, up-estuary transport occurs during flood tide and down-estuary transport occurs during ebb tide.

4 – Summary and Conclusions:

We use a numerical simulation of the Delaware Bay and particle tracking in order to study organismal exposure to neutrally-buoyant and positively-buoyant plastic fields. The

organismal behavior and distribution are based on the dominant zooplankton species in the Delaware Bay, *Acartia tonsa*, but is here referred to as marine organisms both for simplicity and to reflect how these results could also apply to any organism that exhibits passive movement. We find that exposure to plastics changes over time as the marine organisms move in the Delaware Bay. For the neutrally-buoyant plastics field, the location in the bay is the key factor in determining exposure to plastics, with higher exposure levels for organisms in the upper bay. However, exposure can be modified by DVM as it can either reduce local plastics exposure, due to lesser plastics concentrations at depth, or it can influence exposure by either limiting or hastening horizontal movement toward the bay mouth, depending on the tidal phasing of when the organisms are at the surface, where plastics concentrations are lesser. For the surface-trapped plastics field, both the location in the bay, due to the lateral variability in the patchy, inhomogeneous plastics distribution, and the organism behavior are key for determining the exposure to plastics as more plastics accumulate near the mouth of the bay and DVM can fully remove the organism from the plastics field.

We also find that, even for a fixed point in the bay, exposure is variable for both neutrally-buoyant plastics and positively-buoyant plastics. The neutrally-buoyant plastics field is associated with relatively small, regular variations in exposure at a fixed point. The surface-trapped plastics field, however, is associated with sudden large changes in exposure that can exceed 4 orders of magnitude. These high variations also explain the differences between exposure events for the DVM organisms. When these organisms descend to depth, they enter a much slower current regime than that at the surface. This would allow the tidelines with surface-trapped plastics to be either transported away from or to be moved over the organisms

while these organisms are at depth, resulting in either a higher or lower exposure depending on whether the organism surfaces near or away from a tideline.

This proof-of-concept study, while idealized, highlights many important features. First, it highlights the inhomogeneous distribution of surface-trapped plastics and organisms, which can lead to highly variable exposure levels over time. Additionally, the model demonstrates how the movement of organisms and plastics at differing levels in the water column could lead to differing horizontal locations in the estuary, thereby greatly affecting exposure.

As this is a proof-of-concept study, there are several aspects of that model that should be further explored in the future. One such aspect is the buoyancy and size of the plastics. While the assumptions made in this paper are consistent with observational data for the Delaware Bay (Cohen et al. 2019), more work is needed to comprehensively determine size, shape, and density effects on particle transport in estuaries. Additionally, if trying to replicate field data, the effects of model forcings should be further considered, such as wind, variable river discharge, and water-level set-up from passing storms. Another aspect that should be further explored is the plastic scaling. We assume a straightforward plastic distribution using a linear interpolation with salinity for neutrally-buoyant plastics and one source for surface-trapped plastics. The plastic distribution in estuaries is likely to be more complex and could lead to areas of high plastic concentration that are not captured by our model.

Overall, our results indicate that marine organism exposure to microplastics in a dynamic estuarine environment greatly depends on plastic buoyancy effects and the organism's DVM, which need to be considered for comprehensive microplastic impact studies and ecological risk assessment.

Acknowledgements:

This work was supported by Delaware Sea Grant award number NA18OAR4170086 and NOAA Marine Debris Grant NA19NOS9990084. We would also like to thank the anonymous reviewers for their suggestions to improve this text.

Conflict of Interest:

Authors declare no competing financial interest.

References:

Andrady, A. L. (2011). Microplastics in the marine environment. *Marine Pollution Bulletin*, *62*, 1596-1605. https://doi.org/10.1016/j.marpolbul.2011.05.030

Aristizábal, M., & Chant, R. (2013). A numerical study of salt fluxes in the Delaware Bay estuary. *Journal of Physical Oceanography, 43*(8), 1572-1588. https://doi.org/10.1175/JPO-D-12-0124.1

Bikker, J., Lawson, J., Wilson, S., & Rochman, C. M. (2020). Microplastics and other anthropogenic particles in the surface waters of the Chesapeake Bay. *Marine Pollution Bulletin*, *156*, 111257. https://doi.org/10.1016/j.marpolbul.2020.111257

Botterell, Z. L. R., Beaumont, N., Dorrington, T., Steinke, M., Thompson, R. C., & Lindeque, P. K. (2019). Bioavailability and effects of microplastics on marine zooplankton: A review. Environmental Pollution, 245, 98-110. https://doi.org/10.1016/j.envpol.2018.10.065

Brunner, K., Kukulka, T., Proskurowski, G., Law, K. L. (2015). Passive buoyant tracers in the ocean surface boundary layer: 2. Observations and simulations of microplastic marine debris. *Journal of Geophysical Research*, *120*(11), 7559-7573. https://doi.org/10.1002/2015JC010840

Castellano, P. J., & Kirby, J. T. (2011). *Validation of a hydrodynamic model of Delaware bay and the adjacent coastal region* (Res. Rept. CACR-11-03). Newark, DE: Center for Applied Coastal Research, University of Delaware.

Cohen, J. H., Internicola, A. M., Mason, R. A., & Kukulka, T. (2019). Observations and simulations of microplastic debris in a tide, wind, and freshwater-driven estuarine environment: the Delaware Bay. *Environmental Science and Technology, 53*(24), 14204-14211. https://doi.org/10.1021/acs.est.9b04814

Cohen, J. H., & Forward, Jr., R. B. (2009). Zooplankton diel vertical migration: a review of proximate control. *Oceanography and Marine Biology: An Annual Review*, *47*, 77-110.

Cronin, L. E., Daiber, J. C., & Hulbert, E. M. (1962). Quantitative Seasonal Aspects of Zooplankton in the Delaware River Estuary. *Chesapeake Science*, *3*(2), 63-93.

Friedrichs, C. T., & Aubrey, D. G. (1988). Non-linear tidal distortion in shallow well-mixed estuaries: a synthesis. *Estuarine, Coastal and Shelf Science*, *27*(5), 521-545. https://doi.org/10.1016/0272-7714(88)90082-0

Garvine, R. W. (1991). Subtidal frequency estuary-shelf interaction: Observations near Delaware Bay. *Journal of Geophysical Research, 96*, 7049-7064.

Geyer, W. R., Ralston, D. K., & Chen, J.-L. (2020). Mechanisms of exchange flow in an estuary with a narrow, deep channel and wide, shallow shoals. *Journal of Geophysical Research: Oceans*, *125*, e2020JC016092. https://doi.org/10.1029/2020JC016092

Gray, A. D., Wertz, H., Leads, R. R., & Weinstein, J. E. (2018). Microplastic in two South Carolina Estuaries: Occurrence, distribution, and composition. *Marine Pollution Bulletin*, *128*, 223-233 https://doi.org/10.1016/j.marpolbul.2018.01.030

Haidvogel, D. B., Arango, H. G., Hedstrom, K., Beckmann, A., Malanotte-Rizzoli, P., & Shchepetkin, A. F. (2000). Model evaluation experiments in the north Atlantic basin: Simulations in nonlinear terrain-following coordinates. *Journal of Physical Oceanography*, *39*(5), 1077-1096.

Hays, G. C. (2003). A review of the adaptive significance and ecosystem consequences of zooplankton diel vertical migrations. *Hydrobiologia*, *503*, 163-170. https://doi.org/10.1023/B:HYDR.0000008476.23617.b0

Hofmann, E. E., Bushek, D., Ford, S. E., Guo, X., Haidvogel, D., Hedgecock, D., Klinck, J. M., Milbury, C., Narvaez, D., Powell, E., Wang, Y., Wang, Z., Wilkin, J., & Zhang, L. (2009). Understanding how disease and environment combine to structure resistance in estuarine bivalve populations. *Oceanography, 22*(4), 212-231. https://doi.org/10.5670/oceanog.2009.110

Horner-Devine, A. R., Hetland, R. D., & MacDonald, D. G. (2015). Mixing and Transport in Coastal River Plumes. *Annual Review of Fluid Mechanics*, *47*, 569-594. https://doi.org/10.1146/annurev-fluid-010313-141408

Jurisa, J.T., & Chant, R.J. (2013). Impact of offshore winds on a buoyant river plume system. *Journal of Physical Oceanography, 43*(12), 2571-2587. https://doi.org/10.1175/JPO-D-12-0118.1

Kimmerer, W. J., Gross, E. S., & MacWilliams, M. L. (2014). Tidal migration and retention of estuarine zooplankton investigated using a particle-tracking model. *Limnology and Oceanography*, *59*(3), 901-916. https://doi.org/10.4319/lo.2014.59.3.0901

Kukulka, T., Jenkins, R. L., Kirby, J. T., Shi, F., & Scarborough, R. W. (2017). Surface wave dynamics in Delaware Bay and its adjacent coastal shelf. *Journal of Geophysical Research: Oceans*, *122*, 8683-8706. https://doi.org/10.1002.2017JCO13370

Kukulka, T., Law, K. L., & Proskurowski, G. (2016). Evidence for the influence of surface heat fluxes on turbulent mixing of microplastic marine debris. *Journal of Physical Oceanography*, 46, 809-815. https://doi.org/10.1175/JPO-D-15-0242.1

Kukulka, T., Proskurowski, G., Morét-Ferguson, S. E., Meyer, D. W., & Law, K. L. (2012). The effect of wind mixing on the vertical distribution of buoyant plastic debris. *Geophysical Research Letters, 37*(7). https://doi.org/10.1029/2012GL051116

Lampert, W. (1989). The adaptive significance of diel vertical migration of zooplankton. *Functional Ecology*, *3*, 21-27.

Large, W., & Pond, S. (1981). Open ocean momentum flux measurements in moderate to strong winds. *Journal of Physical Oceanography, 11*(3), 324-336.

Law, K. L. (2017). Plastics in the Marine Environment. *Annual Review of Marine Science, 9*, 205-229. https://doi.org/10.1146/annurev-marine-010816-060409

Law, K. L., Morét-Ferguson, S. E., Goodwin, D. S., Zettler, E. R., DeForce, E., Kukulka, T., & Proskurowski, G. (2014). Distribution of surface plastic debris in the eastern Pacific Ocean from an 11-year data set. *Environmental Science and Technology*, *48*(9), 4732-4738. https://doi.org/10.1021/es4053076

Law, K. L., Morét-Ferguson, S. E., Maximenko, N. A., Proskurowski, G., Peacock E. E., Hafner, J., & Reddy, C. M. (2010). Plastic accumulation in the North Atlantic subtropical gyre. *Science*, *329*(5996), 1185-1188. https://doi.org/10.1126/science.1192321

Leandro, S. M., Tiselius, P., & Queiroga, H. (2006). Growth and development of nauplii and copepodites of the estuarine copepod *Acartia tonsa* from southern Europe (Ria de Aveiro, Portugal) under saturating food conditions. *Marine Biology*, *150*, 121-129. https://doi.org/10.1007/s00227-006-0336-y

Lerczak, J. A., & Geyer, W. R. (2004). Modeling the lateral circulation in straight, stratified estuaries. *Journal of Physical Oceanography*, *34*, 1410-1428. https://doi.org/10.1175/1520-0485(2004)034<1410:MTLCIS>2.0.CO;2

Li, M., Cheng, P., Chant, R., Valle-Levinson, A., & Arnott, K. (2014). Analysis of Vortex Dynamics of Lateral Circulation in a Straight Tidal Estuary. *Journal of Physical Oceanography*, *44*, 2779-2795. https://doi.org/10.1175/JPO-D-13-0212.1

Luettich, R. A., Jr., Westerink, J. J., & Scheffner, N. W. (1992). *Adcirc: An advanced three-dimensional circulation model for shelves, coasts, and estuaries. Report 1. Theroy and methodology of ADCIRC-2DDI and ADCIRC-3DL* (Tech. Rep. DRP-92-6, 137 pp.). Vicksburg, MS: Coastal Engineering Center.

MacCready, P., & Geyer, W. R. (2010). Advances in Estuarine Physics. *Annual Review of Marine Science*, *2*(1), 35-58.

McSweeney, J. M., Chant, R. J., Wilkin, J. L., & Sommerfield, C. K. (2017). Suspended-Sediment Impacts on Light-Limited Productivity in the Delaware Estuary. *Estuaries and Coasts*, *40*, 977-993. https://doi.org/10.1007/s12237-016-0200-3

Münchow, A., Masse, A. K., & Garvine, R. W. (1992). Astronomical and nonlinear tidal currents in a coupled estuary shelf system. *Continental Shelf Research*, *12*(4), 471-498. https://doi.org/10.1016/0278-4343(92)90087-Z

Nidzieko, N. J. (2010). Tidal asymmetry in estuaries with mixed semidiurnal/diurnal tides. *Journal of Geophysical Research: Oceans*, *115*, C08006. https://doi.org/10.1029/2009JC005864

Nunes, R. A., & Simpson, J. H. (1985). Axial convergence in a well-mixed estuary. *Estuarine, Coastal and Shelf Science*, *20*(5), 637-649. https://doi.org/10.1016/0272-7714(85)90112-X

O'Donnell, J. (1993). Surface Fronts in Estuaries: A Review. *Estuaries*, *16*(1), 12-39.

Ostle, C., Thompson, R. C., Broughton, D., Gregory, L., Wootton, M., & Johns, D. G. (2019). The rise in ocean plastics evidenced from a 60-year time series. Nature Communications, 10(1), 1622. https://doi.org/10.1038/s41467-01909506-1

ROMS. (2016). ROMS: Technical Documentation. Retrieved from https://www.myroms.org/wiki/Documentation_Portal

Sharp, J. (1983). *The Delaware Estuary: Research as background for estuarine management and development*. Newark, DE: University of Delaware and New Jersey Marine Sciences Consortium.

Shchepetkin, A. F., & McWilliams, J. C. (2005). The regional oceanic modeling system (ROMS): a split-explicit, free-surface, topography-following-coordinate oceanic model. *Ocean Modelling, 9*, 347-404. https://doi.org/10.1016/j.ocemod.2004.08.002

Sommerfield, C. K., & Wond, K.-C. (2011). Mechanisms of sediment flux and turbidity maintenance in the Delaware Estuary. *Journal of Geophysical Research*, *116*, C01005. https://doi.org/10.1029/2010JC006462

Sutton, R., Mason, S. A., Stanek, S. K., Willis-Norton, E., Wren, I. F., & Box, C. (2016). Microplastic contamination in the San Francisco Bay, California, USA. *Marine Pollution Bulletin*, *109*(1), 230-235. https://doi.org/10.1016/j.marpolbul.2016.05.077

US EPA (US Environ. Prot. Agency). (2016). *State of the Science White Paper: A Summary of Literature on the Chemical Toxicity of Plastics Pollution to Aquatic Life and Aquatic-Dependent Wildlife* (Rept. EPA-822-R-16-009). Washington, DC: United States Environmental Protection Agency.

Van Colen, C., Vanhove, B., Diem, A., & Moens, T. (2020). Does microplastic ingestion by zooplankton affect predator-prey interactions? An experimental study on larviphagy. *Environmental Pollution*, *256*, 113479. https://doi.org/10.1016/j.envpol.2019.113479

van Sebille, E., Aliani, S., Law, K. L., Maximenko, N., Alsina, J. M., Bagaev, A., Bergmann, M., Chapron, B., Chubarenko, I., Cózar A., Delandmeter, P., Egger, M., Fox-Kemper, B., Garaba, S. P., Goddijn-Murphy, L., Hardesty, B. D., Hoffman, M. J., Isobe, A., Jongedijk, C.

E., Kaandorp, M. L. A., Khatmullina, L., Koelmans, A. A., Kukulka, T., Laufkötter, C., Lebreton, L., Lobelle, D., Maes, C., Martinez-Vicente, V., Maqueda, M. A. M., Poulain-Zarcos, M., Rodrígues, E., Ryan, P. G., Shanks, A. L., Shim, W. J., Suaria, G., Thiel, M., van den Bremer, T. S., & Wichmann, D. (2020). The physical oceanography of the transport of floating marine debris. *Environment Research Letters*, *15*, 023003. https://doi.org/10.1088/1748-9326/ab6d7d

Vermeiren, P., Muñoz, C. C., & Ikejima, K. (2016). Sources and sinks of plastic debris in estuaries: A conceptual model integrating biological, physical and chemical distribution mechanisms. *Marine Pollution Bulletin, 113*(1-2), 7-16. https://doi.org/10.1016/j.marpolbul.2016.10.002

Warner, J. C., Armstrong, B., He, R., & Zambon, J. B. (2010). Development of a coupled ocean-atmosphere-wave-sediment transport (COAWST) modeling system. *Ocean Modelling, 35*(3), 230-244.

Whitney, M. M., & Garvine, R. W. (2005). Wind influence on a coastal buoyant outflow. *Journal of Geophysical Research*, *110*, C03014. https://doi.org/10.1029/2003JC002261

Whitney, M. M., & Garvine, R. W. (2006). Simulating the Delaware Bay buoyant outflow: Comparison with observations. *Journal of Physical Oceanography, 36*(1), 3-21.

Wong, K. -C., & Münchow, A. (1995). Buoyancy forced interaction between estuary and inner shelf: Observation. *Continental Shelf Research, 15*(1), 59-88.

Wickline, A. (2016). *Seasonal and historical mesozooplankton dynamics in Delaware Bay: an application and optimization of the ZooScan optical imaging tool* (M.S. Thesis). Lewes, DE: University of Delaware

Wright, S. L., Thompson, R. C., & Galloway, T. A. (2013). The physical impacts of microplastics on marine organism: A review. *Environmental Pollution*, *178*, 483-492. https://dx.doi.org/10.1016/j.envpol.2013.02.031

Yonkos, L. T., Friedel, E. A., Perez-Reyes, A. C., Ghosal, S., & Arthur, C. D. (2014). Microplastics in four estuarine rivers in the Chesapeake Bay, U.S.A. *Environmental Science and Technology*, *48*(24), 14195-14202. https://doi.org/10.1021/es5036317